

Exploring Potential Signatures of QGP in UHECR Ground Profiles

Danielle LaHurd^a and Corbin E. Covault^a

^aCase Western Reserve University
10900 Euclid Ave, Cleveland, OH 44106

E-mail: dvl@case.edu, corbin.covault@case.edu

Abstract. In this work we explore the possibility that the formation of Quark Gluon Plasma (QGP) during the first interactions of Ultra High Energy Cosmic Rays (UHECRs) may result in observable signatures in ground profile and shower particle composition that could conceivably be detectable by an air shower array experiment such as the Pierre Auger Observatory. Knowledge of whether QGP formation affects the properties of UHECR development will further the understanding of both UHECR behavior and high energy hadronic interaction behavior. We find that for the vast majority of showers signals of QGP do not manifest themselves in ways that are observable, but on rare occasion, such as within deeply penetrating showers, observable signals can be seen. Results show potential for QGP detection at 100 PeV initial energy at an initial interaction event height of 12 km through a μ^\pm excess at 10 GeV between 100 - 300 m from the shower core favoring QGP forming events. In contrast, higher initial interaction heights of 24 and 36 km at 100 PeV initial energy show no significant potential for QGP detection. Unfortunately at present, the 12 km observable signals cannot be seen with current detectors, such as the Pierre Auger Observatory[1]; however, there may be potential for detection in future experiments.

ArXiv ePrint: [1707.01563](https://arxiv.org/abs/1707.01563)

Contents

1	Introduction	1
2	Methodology	2
2.1	Simulation Models	3
2.1.1	QGP Event Selection	3
3	CORSIKA Simulation	5
3.1	“Head” and “Body”	6
3.1.1	Converting to CORSIKA Format	6
3.2	Analysis	6
4	Results	8
4.1	Initial height: 12 km	8
4.1.1	Initial height: 12 km Discussion	10
4.2	Initial height: 24 km	11
4.3	Initial height: 36 km	11
5	Discussion	12

1 Introduction

After a UHECR penetrates the atmosphere, it has increasing chances for interaction as it propagates. Upon the inevitable UHECR-Air collision, its center-of-mass energy is of equivalent or greater magnitude ($\sqrt{s_{NN}} \sim 100$ TeV) to what is currently being run at the LHC. As a result, UHECRs and hadronic interactions are fundamentally linked.

It is hypothesized that a new state of matter may exist at very high energy density, where quarks and gluons become asymptotically free. This state is called a Quark Gluon Plasma (QGP), in analogy to electromagnetic behavior of high-temperature collections of charged particles. A QGP is defined as a local thermal equilibrium, whereby quarks and gluons are deconfined from hadrons and manifest color degrees of freedom on nuclear scales rather than nucleon scales [3]. The quarks and gluons in a QGP exhibit fluid-like behavior - “flows” - rather than simpler scatterings that occur at lower energy density [12]. Signatures of “flow” have been reported experimentally from $p + Pb$ collisions at $\sqrt{s_{NN}} = 2.76$ TeV collisions at the LHC [6] [14], and there has been recent evidence of a small QGP formation in ${}^3\text{He} + \text{Au}$ collisions at RHIC at $\sqrt{s_{NN}} = 200$ GeV [4].

Since there is recently increasingly strong evidence of QGP formation at collider energies used at RHIC and the LHC, and UHECR collision energies are an order of magnitude higher (~ 100 TeV), it stands to reason that, although the interacting hadrons may be lighter, it is plausible that QGP formation may be occurring during the initial UHECR collision.

We note that the question of potentially observable effects of QGP in UHECRs has been asked in prior work [21] using a simplified, two-parton, QGP model, as well as in work [5] done using a String Percolation Model. However, we believe ours is the first study using up-to-date hadronic interaction models, including hydrodynamic flow behavior, since first QGP observation in 2005. Knowledge of whether QGP formation affects the properties of

UHECR development will further the understanding of both UHECR behavior and high energy hadronic interaction behavior.

2 Methodology

Our approach is to use simulation studies of high energy interactions and air shower propagation in the atmosphere to explore the feasibility that an observational signature indicating the formation of QGP may be detected based on measurements of ground particles. In order for a compelling QGP signal to be measured, several steps in sequence need to occur:

1. QGP must be created as a result of first interactions between UHECRs and air molecules at a sufficient rate,
2. A sufficient fraction of each QGP must result in child particles with characteristics uniquely indicative of QGP, for example, multiplicity (N) and flow,
3. A sufficient fraction such events must generate a particle cascade where some imprint of the QGP signature remains in some detectable form in the properties of particles arriving to the ground, and finally,
4. The distinguishing signatures of ground particles must be measurable experimentally and must occur at a rate high enough to be detected against any background due to non-QGP cosmic ray showers fluctuating so as to mimic the specified signal.

Here, we examine in some detail the plausibility for the first three steps indicated above. We begin by applying hadronic models to primary interactions which allow for the generation of QGP. We then select a subset of these interactions where QGP signatures in child particles can be most clearly discerned, operating under the assumption that only events that generate clear QGP signatures in the first interaction have any chance to imprint a measurable signature on the resultant ground particles. Only the most promising subset of interactions are then fed into a full air shower simulations which propagate particles to the ground. Since the air shower simulations are most time-consuming computationally, we inject selected showers into the atmosphere at discrete depths corresponding to three heights: 12 km, 24 km and 36 km spanning a range shower penetration. Finally we examine distributions of ground particles for signatures of QGP in the selected air showers relative to a matched set of non-QGP initiated showers.

Our central aim is not to assess the absolute detectability of QGP in the context of realistic distributions of cosmic ray and air shower properties, but rather to assess if any discernible signal might be seen in ground particles even under optimistic assumptions where showers are pre-selected with favorable first interactions taking place deep in the atmosphere. We emphasize that here that we have not completed any study to carefully infer the rate at which QGP signatures might appear in real air shower ground particles generated from real UHECRs. Also here we make no attempt to address the extent to which non-QGP initiated showers can fluctuate so as to yield a background of air showers that mimic QGP signatures. Such studies will require substantially greater computational resources that have been applied here.

2.1 Simulation Models

In order to explore the effects of QGP formation during the initial atmospheric interaction on shower evolution selection criteria are used on simulated events in order to select for promising QGP candidate events. A discussion [24] was consulted to determine model strengths in simulating and reproducing flow in $p+Pb$. The two high-energy hadronic interaction models used for this discussion are QGSJETII-04 [16][13] and EPOS-LHC [25][20][19], both tuned to the most recent LHC data. QGSJETII-04 does *not* include hydrodynamic interactions that may occur within the initial hadronic collision during a QGP formation. For this reason, we use QGSJETII-04 as the “non-signal” comparison for the purposes of this discussion. Additionally, due to its slightly faster simulation speed, we also use QGSJETII-04 for the air shower propagation portion of the simulation.

EPOS-LHC [19] is based on the Parton Gribov-Regge Theory [8] and includes a parametrized version of hydrodynamic modeling, replicating QGP effects. A version of EPOS, EPOS 3.x [23], exists with full 3D+1 viscous hydrodynamic simulation. However, on consultation with T. Pierog [18], it was determined the compute time required for simulating initial events in EPOS 3 would be too extreme for the purposes of this study, with times estimated on the order of a month per each initial event and no guarantee that the resulting simulated event would have all the features desired for study. Since the full hydrodynamic simulation of EPOS 3 is outside our currently available computing resources, the parametrized hydrodynamics of EPOS-LHC are instead used for simulating the hydrodynamic, or ‘QGP signal’, initial events.

We separate the modeling of the initial event from the atmospheric propagation simulation occurring subsequent from the initial interaction. Additionally, we use the same model for said atmospheric propagation for both ‘signal’ and ‘non-signal’ events to limit the search for differences between the ‘signal’ and ‘non-signal’ to differences within the initial interaction rather than dealing with additional atmospheric propagation differences between models.

Specifically, the initial hadronic interactions for both models, EPOS-LHC and QGSJETII-04, are *not* simulated in the cosmic ray propagation simulation package, CORSIKA [11], but are instead generated in a separate program module called CRMC (Cosmic Ray Monte Carlo) [22], allowing for the simulation of large numbers of initial events. Selection cuts are made on the CRMC simulated events before continuing simulation in CORSIKA.

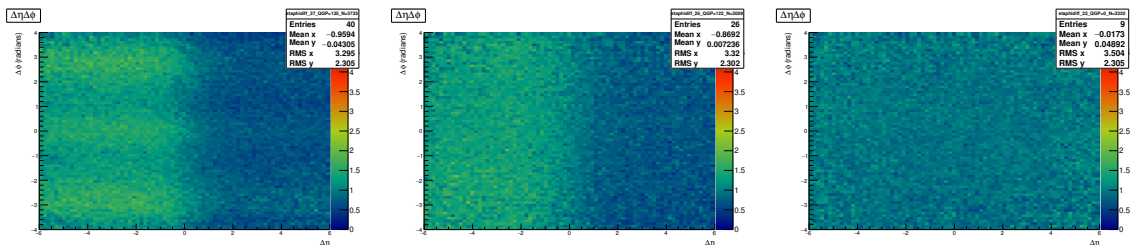
2.1.1 QGP Event Selection

Certain selection cuts on initial collision events have been made in order to ensure a decent sample size of potential QGP-positive initial interactions. All initial interaction events were simulated in 50 event batches using EPOS-LHC and CRMC v1.4 and v1.5.5. The simulations were of vertical Neon (Ne) primaries at 100 PeV (0.1 EeV) hitting a Carbon (C) target at rest ($\sqrt{s_{NN}} \approx 3$ TeV comparable to LHC energies). Neon was chosen due to two factors: simulation time and nucleon density. Iron (Fe) and Silicon (Si) primaries were also tested. While an iron primary would be the ideal for testing behaviors and observables due to increased density, the computing time required with our current available resources made it untenable. A neon primary sits in the “sweet spot” of compute time for available resources, around 2 - 4 days per simulation, with a reasonable probability for observing QGP behavior in initial interactions while still being a potential, if rare, cosmic ray primary candidate. Protons, while having the fastest compute time, only demonstrate QGP behaviors in the most extreme high multiplicity circumstances. These high multiplicity ($N > 1800$ particles)

initial events occur in $< 1\%$ of simulated proton events. The initial energy of 100 PeV was also chosen due to compute time restrictions.

We are aware that collisions of 100 PeV cosmic rays may probe just the onset of quark deconfinement, and air shower signals for the formation of a quark gluon plasma could still appear at much higher energies. It is important to probe the entire energy parameter space from the onset of deconfinement and higher energies to determine what effects deconfinement has on shower evolution and development.

Before any full $Ne + C$ simulation was done, a small series of test showers were run to compare outputs between EPOS-LHC and QGSJETII-04. Figure 1 shows the azimuthal angular and pseudorapidity difference of pairs of particles produced in hadronic interactions simulated with and without collective effects. The color code shows the number of particle pairs found for a given difference in azimuthal angle and pseudorapidity. EPOS-LHC events showed signs of collective behavior (1a and 1b), while, as expected, the QGSJETII-04 events did not show the same collective behavior (figure 1c). Similarly, when QGP effects are turned off in EPOS, the results are similar to the QGSJETII-04 output [15].



(a) EPOS-LHC initial condition with QGP effects present. (b) EPOS-LHC initial condition without full QGP presence. (c) QGSJET initial condition. Note no collective behavior at any $\Delta\eta$ or $\Delta\phi$.

Figure 1: Simulated particle distributions for pairs of particles produced in under different hadronic interactions models as a function of both pseudo-rapidity difference $\Delta\eta$ and azimuthal angle difference $\Delta\phi$. The color code shows the number of particle pairs found for a given $\Delta\eta$ and $\Delta\phi$. All events have ~ 3000 particles.

All QGP candidate events are selected to have more than 2000 particles at initial freeze-out. This requirement selects for high multiplicity events and reduces false positives in $\Delta\eta\Delta\phi$ graphing. Events with lower than 2000 freeze-out particles generally lack sufficient statistics to discern any flow-like effects. Events with greater than 4000 particles at freeze-out were also cut, due to both the rarity of these events ($< 0.004\%$) and difficulties in observing possible flow behavior without additional pseudo-rapidity (η)¹ cuts via the large number of particles obscuring the flow effects. In principle, additional η or p_T cuts could be made to view flow effects within the high multiplicity candidates; however, for this analysis, these cuts were not made.

The QGSJETII-04 “non-signal” initial events are also given the same multiplicity cut, limiting the events to those with $2000 < N < 4000$. QGSJETII-04 initial events tend to have higher initial multiplicity due to the lack of hydrodynamical effects and QGP density

¹ $\eta = -\ln\left(\tan\frac{\theta}{2}\right) = \frac{1}{2}\ln\frac{|\mathbf{p}|+p_z}{|\mathbf{p}|-p_z}$

Cut Applied	Number of Events	Percent Remaining
Total events simulated	3550	100%
Impact Parameter < 5 fm	1918	54%
Multiplicity cut of $N \geq 2000$	538	15%
Multiplicity cut of $N < 4000$	524	14.7%
Cosine fit $v_2 > 0.02$ and visible ‘ridges’	51	1.4%

Table 1: The number of EPOS-LHC events simulated for potential QGP events and the efficiency of applied selection cuts.

induced suppression. We limit the multiplicity of QGSJETII-04 events to ensure similar initial conditions to those of the QGP ‘signal’ events.

The impact parameter, or separation of the centers of the two nuclei when they collide, is provided by the HepMC [7] output of a CRMC simulation. Only QGP candidate events that have a low impact parameter, i.e. high nucleus overlap, are selected for this study as low impact parameter correlates strongly with high multiplicity. The impact parameter chosen was $b < 5$ fm, which corresponds to roughly 0%-15% centrality (85% - 100% nucleus overlap).

In order to obtain events with high “flow” corresponding to a possible QGP signature, the events are graphed on a $\Delta\phi$ vs. N graph, then fitted with a Fourier cosine function describing flow:

$$f(\Delta\phi) = 1 + \sum_{n=1}^3 2c_n \cos(n\Delta\phi)$$

It is the v_2 ($n=2$) term that is of most interest, as it is a sign of strong collective behavior that is influenced positively by the presence of a QGP. Fits were used to select for strong QGP candidate events. If the v_2 coefficient, corresponding to elliptic flow, was below 0.02, the event was rejected, as lower v_2 values correspond to weaker flow effects (low initial anisotropy). This fitting selection process ignores fit errors and is only used as a framework for selecting potential QGP events.

The pass rate with all cuts is about 1.4%. Table 1 shows a summary of the selection cuts applied and the overall efficiency.

3 CORSIKA Simulation

While EPOS-LHC and QGSJETII-04 are used for the high energy hadronic interaction simulations, it is the program CORSIKA [11] that takes these models and uses them to model the propagation of particles through the atmosphere. The version used for the hadronic interaction comparison simulations at the time of the discussion is CORSIKA v74004. CORSIKA transitions to a lower energy interaction model, FLUKA (v2011.2) [9][10], for particle simulations when the energy of individual particles falls below 100 GeV (configured at time of simulation).

Thinning in CORSIKA is the process by which computing time is shortened by only following one particle from a cascade below a certain energy rather than every particle individually. Thinning does not preserve flavor counts or baryon numbers [18], therefore care must be taken when deciding the thinning range so as not to lose valuable data. All CORSIKA showers simulated at 100 PeV were thinned at the 10 GeV level. There is assumed to

be no discernible signal in the particles below 10 GeV as additional atmospheric interactions and secondary showers will have clouded the signal.

3.1 “Head” and “Body”

For the “head” or initial interaction, EPOS-LHC and QGSJETII-04 initial events are chosen, as described above in section 2.1.1, and formatted into a CORSIKA readable format.

For the air shower simulation, or “body”, the QGSJETII-04 model was chosen for atmospheric simulation of both initial interaction models. This is to allow for only the initial interaction type to influence the developments within the air shower and allow for more direct comparisons. QGSJETII-04 was chosen over EPOS-LHC for the “body” simulation as it requires slightly less time for simulation. All showers were simulated using the same version of CORSIKA(v74004) and FLUKA to reduce systematic errors.

3.1.1 Converting to CORSIKA Format

As the shower is not being generated internally by CORSIKA, an initial height from the detector plane must be provided for the air shower simulation to begin. Many, very thinned, test showers have been simulated in CORSIKA using proton, carbon, and iron primaries in order to determine the typical initial collision height. For this discussion, the initial collision heights have been chosen at discrete values of 12, 24, and 36 kilometers. For detectability, 12 km potentially shows the most signal originating from the initial collision due to less atmosphere attenuation since first interaction. However, as seen in figure 2 with neon primary interaction heights, it would be extremely uncommon to see an air shower, especially one of somewhat heavier composition such as the neon primaries used, originating at such an extreme atmospheric penetration depth. Interactions set to 24 km represent a value close to the average expected initial height of a shower with a composition near carbon or neon mass, and 36 km represents a high starting-elevation shower. A total of 51 showers have been simulated for each model (102 total showers) for this discussion, with 17 showers generated at each of the three initial heights for both models.

3.2 Analysis

The CORSIKA output files are processed, using C++ scripts, into a ROOT format file consisting of compact particle data such as position, species, generation, time of impact, and momentum.

During analysis we make an energy cut of all particles below 10 GeV. Most particles below 10 GeV result from secondary showers and decays which can wash out potential signals from initial interactions that we wish to examine. Additionally, making the cut at 10 GeV allows us to eliminate particle weights introduced by CORSIKA through simulation thinning. The removal of the weighted particles can be beneficial as the thinning and weighting of particles, while vastly speeding up simulation time, only preserves energy and not baryon or lepton numbers [18]. By not preserving baryon and lepton numbers amongst the weighted particles, the particle species abundances may be altered in a non-physical way and may hide potential differences between the evolution of the two initial interaction types.

The 17 simulations for each model and height are averaged and normalized before comparison to obtain a single distribution for initial interaction model comparison purposes.

One of the ways we compare the two interaction models is through taking the difference between the normalized distributions. This provides a way to look for QGP dependent excesses or deficiencies, after atmospheric evolution. In order to determine the significance

100 PeV Neon First Interaction Height

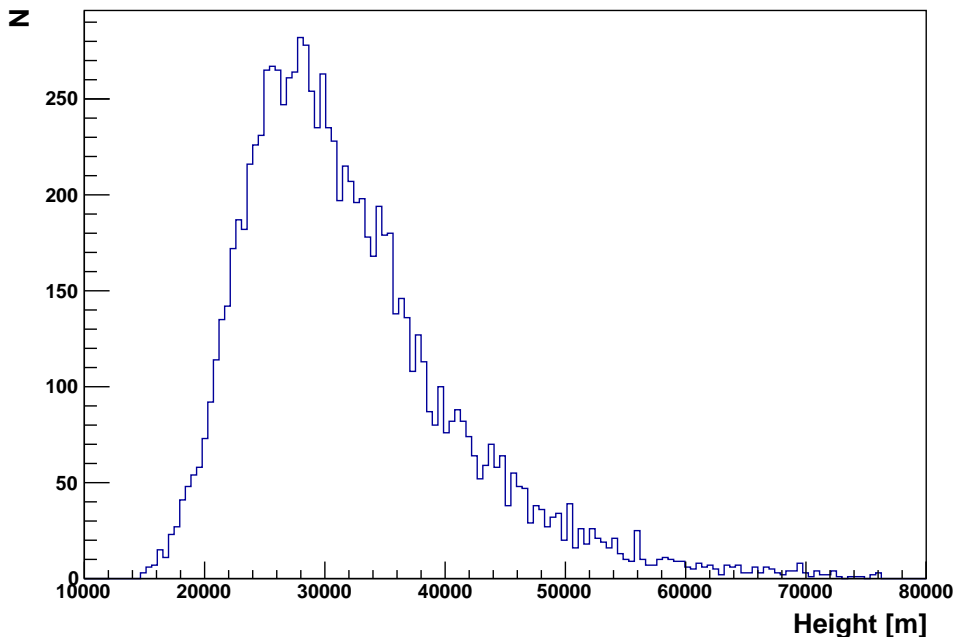


Figure 2: Graph initial interaction height of 100 PeV neon primary showers through 10000 CORSIKA simulations.

of any differences between the QGP and non-QGP results, we divide the differences by the propagated errors of the difference.

$$\mathcal{R} \equiv \frac{\langle N_{QGP} \rangle - \langle N_{noQGP} \rangle}{\sigma}$$

Here \mathcal{R} is the “residual excess”, a measure of the number of standard deviations the difference deviates from a null-hypothesis scenario where both QGP and non-QGP initiated air showers produce the same results, and σ is the RMS uncertainty in the difference between QGP and non-QGP values.

The statistical significance of any one difference is, of course, diluted by the fact that we are searching for a range of different potential signatures. Although the “trials factor” is difficult to estimate, *a posteriori*, we conservatively expect our study to correspond to several hundreds of independent searches. For the purposes of initial analysis, we therefore assign an \mathcal{R} value greater than 3σ as a cause for interest, and assign an \mathcal{R} value of greater than 5σ to represent a likely compelling physical difference between the models. We plot distributions of \mathcal{R} for various different measurements. A distribution centered near zero, signifies that both initial interaction models evolve similarly, or at least do not display significant differences after the initial interaction. If the distribution deviates far from zero, or there are bins residing significantly outside the central collection, there may be an excess in favor of either the QGP (positive) or non-QGP (negative) events.

Additionally, we perform a histogram comparison between 1D variables of QGP and non-QGP modeled events using the χ^2 test of homogeneity [17]. We examine the resulting normalized residuals, i.e. the residuals divided by their standard deviation, from the comparison. If QGP formation has no detectable influence on shower development the residuals

should remain distributed at or near zero. Should any residuals bin deviate strongly from zero, it indicates a potential region where the presence of QGP during the initial collision has influenced shower development. The magnitude of the residuals' deviation from zero scales with, but is not equivalent to, the significance of said deviation.

4 Results

For the presented results we will primarily focus on the 12 km simulated events, as both the 24 and 36 km events show little differences between QGP (EPOS-LHC) and non-QGP (QGSJETII-04) models with the number of events simulated.

4.1 Initial height: 12 km

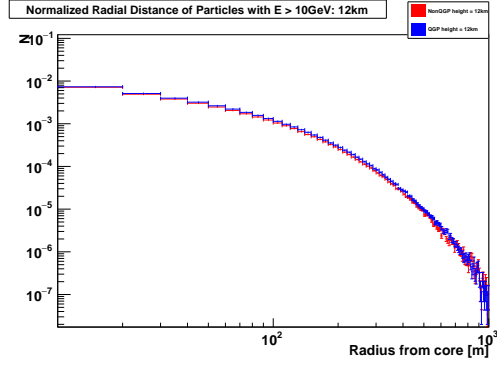
Due to the depth of atmospheric penetration required, a 12 km initial (first interaction) height is an extremely unlikely condition for a Ne, or heavier, primary at 100 PeV. However, examining results at this height provides a informative tool for determining whether viewing QGP effects from the initial interaction is feasible after traversing the atmosphere, or if any potential signal will be eliminated by the numerous interaction lengths traveled. The 12 km sample represents an overly optimistic sample which is the most favorable for the detectability of QGP signature observables. Should no observables be present on the ground after the comparatively short distance of 12 km there will be little hope of finding detectable observables at the higher, more realistic, initial interaction heights of 24 and 36 km.

We examine the radial distribution of particles from the 12 km events for any differences between the distributions of the QGP and non-QGP 'headed' showers. Upon viewing this radial distribution for all tracked particles (figure 3a) we note that QGP (blue) events demonstrate an excess of particles at a 100 m distance from the core. This is difficult to see in the initial log-log comparison, however, until we examine the residuals (figure 3b) comparing the QGP results to the non-QGP results. In the residuals, the QGP excess (positive) is clearly visible from 50 m up to about 300 m. This difference appears to be significant (figure 3c) as there are multiple significance bins exceeding 5σ . Additionally, the significance distribution trends towards positive significance, indicating a overall QGP excess.

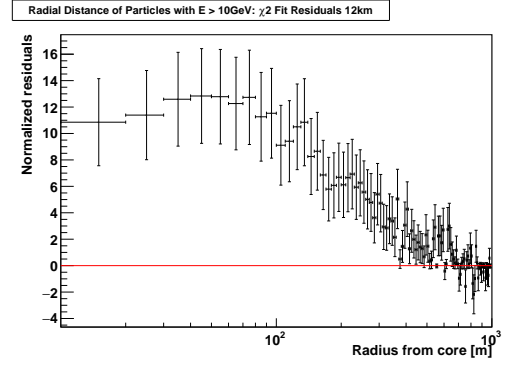
Examining a top-down view of the particle distribution, this QGP-favored excess between 50 m and 300 m remains significant when distributed across the azimuthal bins (figure 4a). The significance values from this distribution (figure 4b) also exceed 5σ . There may be an event-to-event azimuthal clustering; however, this was not studied in this discussion.

Attempting to untangle which particles are contributing to the QGP-favored excess, we examine particle distributions separately based on particle species. The muon profile (figure 5a) displays an excess in favor of QGP. This excess is once again corroborated by the residuals (figure 5b) exhibiting an excess of μ^\pm in favor of QGP between 50 and 300 m. This excess is not as statistically significant (figure 5c) as that seen in the full particle distribution but does contain a number of bins with 5σ significance. On examination, the remaining individual particle species radial distributions show little to no differences between the two models. Therefore, we conclude that the muons dominate the apparent QGP-favored particle excess seen a 50 - 300 m from the core.

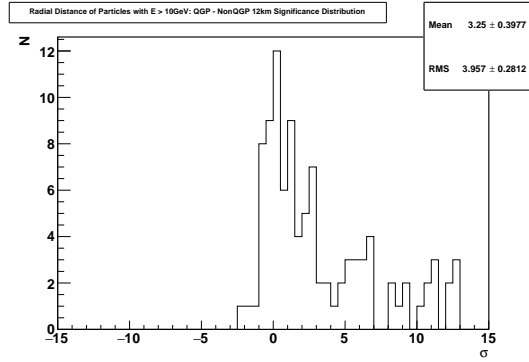
As there appears to be a potential signal in muons for differentiating QGP and non-QGP showers, we examine particle species abundances within the entire ground profile for other possible difference between the models. A normalized count of particle species (figures 6a and 6b) shows a significant difference between the two models for muons and EM. There is



(a) Normalized radial distribution: QGP excess near 100 m.

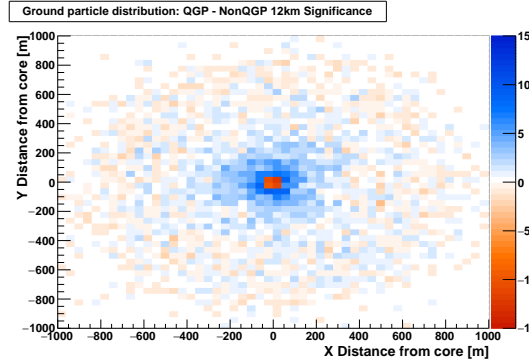


(b) Normalized residuals: QGP excess up to 300 m.

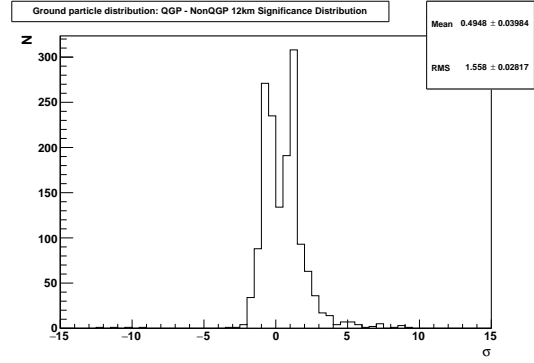


(c) Significance values: Centered on the positive axis; multiple bins are above 5σ .

Figure 3: Radial distribution comparison of all particles with energy exceeding 10 GeV between QGP and non-QGP events with an initial interaction height of 12 km.



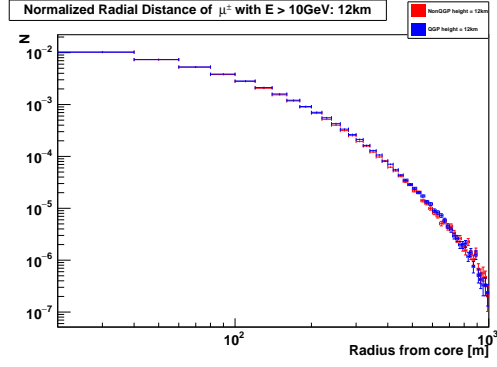
(a) Significance(σ) of the difference of normalized counts by (x, y) .



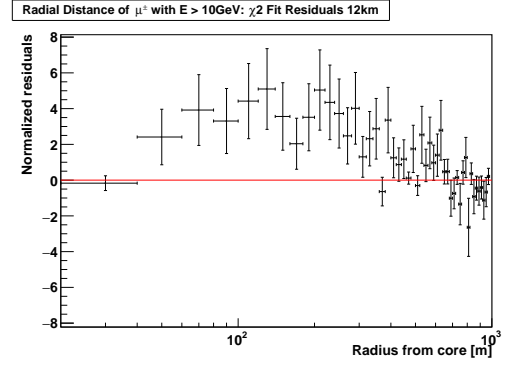
(b) Distribution of significance values of the difference of normalized counts.

Figure 4: Particle distribution (x, y) with energy exceeding 10 GeV and an initial interaction height of 12 km. Significance favoring QGP is positive(blue) and non-QGP is negative(red)

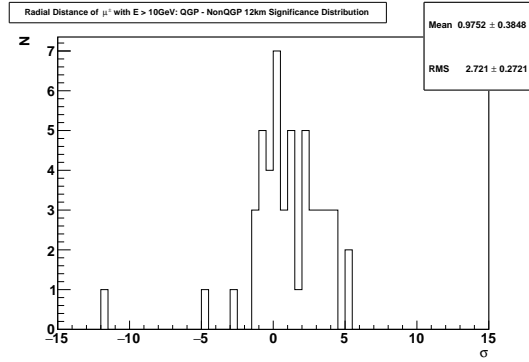
little difference between QGP and non-QGP for the other tracked particle species. The EM (γ, e^\pm) excess strongly favors non-QGP events and μ^\pm excess strongly favors QGP events.



(a) Normalized radial distribution: QGP events are in blue and non-QGP events are in red.

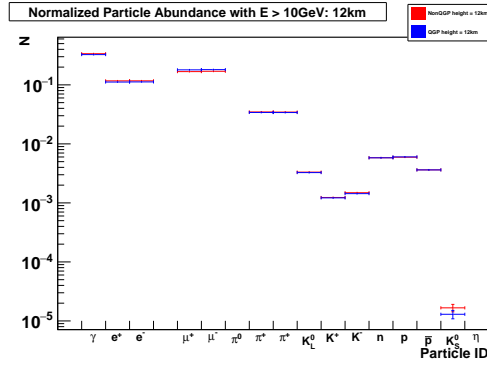


(b) Normalized residuals: QGP-favored excess between 50 and 300 m.

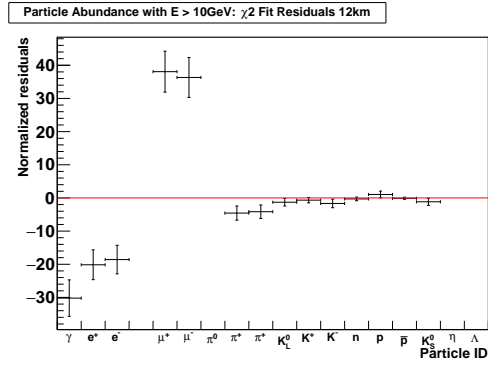


(c) Significance values

Figure 5: Radial distribution comparison of μ^\pm with energy exceeding 10 GeV between QGP and non-QGP events with an initial interaction height of 12 km.



(a) Normalized counts of particle species. QGP events are in blue and non-QGP events are in red.



(b) Normalized residuals comparing particle species.

Figure 6: Comparison of particle species counts and significance with energy exceeding 10 GeV and an initial interaction height of 12 km.

4.1.1 Initial height: 12 km Discussion

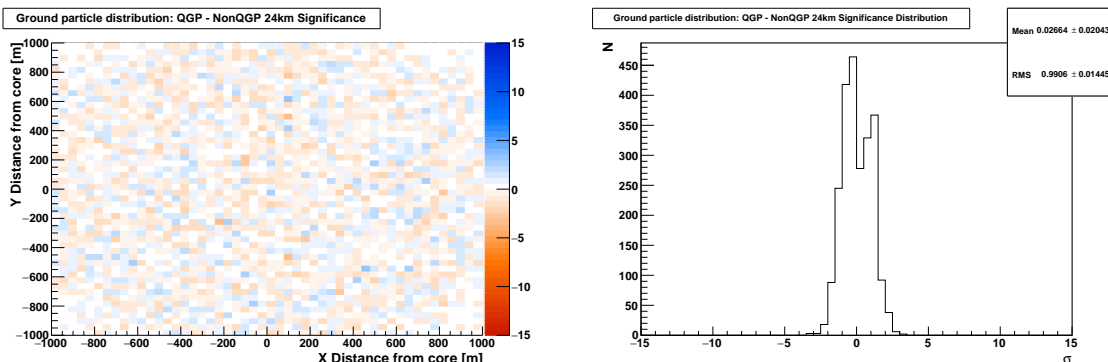
There appears to be a significant difference, especially in the radial particle distribution, in the muon and EM output between the QGP and non-QGP ‘heads’ at 12 km. For the non-QGP ‘headed’ events, there is a e^\pm excess seen within the core region when compared to

QGP headed events. However, there is no current detector capable of measuring the direct shower core output due to the required fine-grain surface detector spacing of $\sim 100\text{ m} - 300\text{ m}$. As such, an e^\pm core excess or deficiency cannot be used as a signature to determine whether an initial event has formed QGP using previously collected data from experiments past or existing, such as Auger.

As for muons, there is a significant difference between the initial interaction model outputs when viewing the area between 50 and 300 m from the core. However, this is only apparent when comparing the discrepancy to the outer regions of the ground profile, where both models are identical. While the spacing of currently existing detectors is not ideal, this signature is potentially detectable if one uses a tightly clustered detector with $\sim 100\text{ m}$ spacing. To search for a QGP signature, one would have to compare the peripheral of the shower's ground profile with the profile of the 50 to 300 m region and find an anomalous excess of particles in comparison to other shower profiles. This could be made easier with the addition of scintillation panels to water Cherenkov surface detectors to better separate muon particle detections from electron detections.

4.2 Initial height: 24 km

For 24 km initial heights, looking at the top-down view of the particle distribution (figure 7a) there appears to be no evidence of excess. In fact, the (x, y) distribution of all particles exceeding 10 GeV, with a 24 km initial height, appears to show no difference between the two models in particle count. This is confirmed by the near-Gaussian distribution of the significance values in figure 7b.



(a) Plot of the significance of the difference in particle count on an $x - y$ plane. There is no favoring of either model present.

(b) Plot of significance value distribution. The values are centered on zero with no deviations outside 3σ favoring one side over the other.

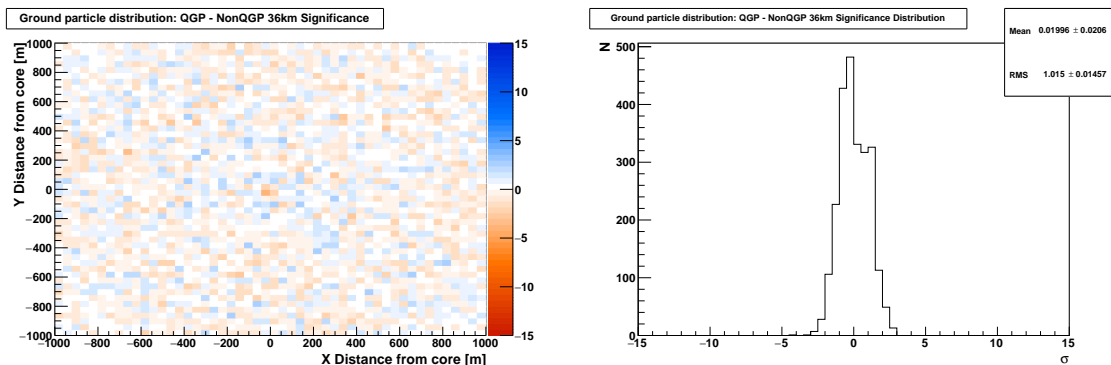
Figure 7: Significance of the difference in distribution of all particles with $E > 10\text{ GeV}$ between QGP and non-QGP events with initial height of 24 km. Positive (blue) signifies a distribution in favor of QGP, while negative (red) signifies a distribution in favor of non-QGP.

4.3 Initial height: 36 km

Any differences between QGP and non-QGP events as measured from the ground particle profile (figures 8a and 8b) at a 36 km initial height appear to be statistically negligible and similar to the 24 km radial distribution discussed previously. Neither figure demonstrates a favoring of one model over the other but rather display an extreme similarity between a

QGP initiated shower and a non-QGP initiated shower. This may be a result of too much time, and/or too many interaction lengths, since first interaction eliminating any perceivable differences.

Unfortunately, the lack of statistically significant effects at 36 km is discouraging for prospects of detecting QGP in real UHECR air showers as a 36 km initial height is many times more likely to occur than one at 12 km. This is especially true with the penetration potential of heavier primaries at 100 PeV, which would be more likely to have QGP formation during initial collision due to containing more interacting nucleons. Ironically, the most favorable conditions for QGP formation occur with the least likely ability for detection, as neon and similar weighted primaries are most likely to interact at a higher elevations.



(a) (x, y) plot of the significance (σ) of the difference in distribution. Note the randomness of the distribution, signifying no favoring of either model.

(b) Plot of the significance distribution. There are no outliers and the significance is centered near zero, implying similar distributions.

Figure 8: Significance of the difference in distribution of all particles with $E > 10$ GeV between QGP and non-QGP events with initial height of 36 km. Positive (blue) signifies a distribution in favor of QGP, while negative (red) signifies a distribution in favor of non-QGP.

5 Discussion

The aim of this discussion is to determine if there exist effects on the ground profile and particle composition of a UHECR air shower due to the formation of QGP during the initial interaction of the UHECR on the atmosphere. The knowledge of whether QGP formation affects the properties of UHECR development would enhance understanding of both UHECR and high energy hadronic interaction behaviors.

Based on the results, the conclusion we reach is, in all practicality, detecting whether QGP has formed within a UHECR is extremely challenging. While there is potential in the 12 km results, more simulated events are needed to verify the extent to which the features seen in the 12 km results remain both present and detectable. With 102 total events simulated, and only 34 at each height, a statistical anomaly within in a single event can alter the perceived results. A more reasonable number of simulations for review would on the order of 100 simulated events per model at each height, thereby limiting the effects of anomalies to 10% or less rather than a 25% effect with the current number of events. Simulating on the order of 1000 events per height and model would only be feasible with supercomputing resources, but would limit the effects of any outlier or anomalous events to $\sim 3\%$.

We must also consider the extreme rarity of a QGP formation event occurring. Via our selection methods, a QGP with potentially detectable properties, e.g. strong hydrodynamic flow and reasonable multiplicity, has a $\sim 1.4\%$ chance of occurring with a neon primary at 100 PeV. These chances are lower for lighter primaries due to fewer interacting nucleons limiting chances for high multiplicity.

Moreover, the probability of a primary particle penetrating deeply enough to have a 12 km initial height is quite small. Based on the height distribution presented in figure 2 for a neon primary at 100 PeV, a 12 km initial height for particles of similar mass is a very rare occurrence with only a 3.18% chance for neon to penetrate deeper than 20 km and a 0.15% chance below 16 km. As a reminder, the 12 km height was primarily chosen as a ‘proof of concept’, whereby a lack of any observables at said height would prove that QGP formation is undetectable in UHECRs.

Therefore, due to the combination of both the rarity of detectable events and the lack of detectability at higher elevations, we must conclude the possibility of observing QGP formation from a UHECR is very small, below a 0.0021% chance per shower, at 100 PeV with a neon or similar mass primary event with an ideal (simulated) detector that records all ground particles.

Although possible detectability is slim at a less than 0.0021% chance per shower, with the upcoming Pierre Auger Observatory upgrade [2] there is potential for detecting deeply-penetrating, QGP-forming, showers. The upgrade adds an additional scintillation panel on top of the currently existing Auger water Cherenkov surface detectors, allowing for more accurate electron and muon discrimination, to a resolution of 15% or better in determining the number of muons [2]. Additionally, the upgrade allows for measurement of shower properties nearer the shower core due to reducing the number of saturated PMTs, from a 1000 m radius to 300 m. The now 300 m radius lies within the potential signal region produced in the simulated QGP-forming events.

As seen from the 12 km results, the finer spacing and muon discrimination in the Pierre Auger upgrade may be enough to detect signs of QGP formation, as the region where signals appear is muonic at 300 m from the core. Care must be taken to select for the deepest penetrating showers which can be inferred either from coincidental fluorescence measurements or through lateral density profiles. Confirmation of results may be limited, however, due to the rarity of the specific conditions required for detectability.

For example: An effective area of the Pierre Auger Observatory Infill (where the spacing between detectors is reduced from 1.5 km to 750 m) region of about 50 km² would yield approximately 100,000 events during a 5-year operating window. At a 0.0021% rate, this would result in about 2 QGP-detectable events based on selection cuts. Although this is in principle a detectable number of events, the rarity of QGP means that selection cuts against non-QGP showers must have very high rejection factors.

Acknowledgments

This discussion was made possible by NSF grant PHY-1207523. D. LaHurd acknowledges the support of the Timken Fellowship at Case Western Reserve University. Data analysis was made possible in part by CRMC[22]. We acknowledge very helpful discussions with and guidance from T. Pierog. We are grateful for editorial and scientific comments and suggestions on the manuscript from J. Matthews and other members of the Pierre Auger Collaboration.

References

- [1] Alexander Aab et al. The Pierre Auger Cosmic Ray Observatory. *Nucl. Instrum. Meth.*, A798:172–213, 2015.
- [2] Alexander Aab et al. The Pierre Auger Observatory Upgrade - Preliminary Design Report. (arXiv:1604:03637), 2016.
- [3] John Adams et al. Experimental and theoretical challenges in the search for the quark gluon plasma: The STAR Collaboration’s critical assessment of the evidence from RHIC collisions. *Nucl. Phys.*, A757:102–183, 2005.
- [4] A. Adare et al. Measurements of elliptic and triangular flow in high-multiplicity $^3\text{He}+\text{Au}$ collisions at $\sqrt{s_{NN}} = 200$ GeV. *Phys. Rev. Lett.*, 115(14):142301, 2015.
- [5] J. Alvarez-Muniz, L. Cazon, R. Conceicao, J. Dias de Deus, C. Pajares, and M. Pimenta. Muon production and string percolation effects in cosmic rays at the highest energies. (arXiv:1209.6474), 2012.
- [6] Serguei Chatrchyan et al. Observation of long-range near-side angular correlations in proton-lead collisions at the LHC. *Phys. Lett.*, B718:795–814, 2013.
- [7] Matt Dobbs and Jorgen Beck Hansen. The HepMC C++ Monte Carlo event record for High Energy Physics. *Comput. Phys. Commun.*, 134:41–46, 2001.
- [8] H.J. Drescher, M. Hladik, S. Ostapchenko, T. Pierog, and K. Werner. Parton-based Gribov-Regge theory. *Physics Reports*, 350(24):93 – 289, 2001.
- [9] A. Fasso et al. The Physics models of FLUKA: Status and recent developments. *eConf*, C0303241:MOMT005, 2003.
- [10] Alfredo Ferrari, Paola R. Sala, Alberto Fasso, and Johannes Ranft. FLUKA: A multi-particle transport code (Program version 2005). (Report: CERN-2005-010, SLAC-R-773, INFN-TC-05-11), 2005.
- [11] D. Heck, G. Schatz, T. Thouw, J. Knapp, and J. N. Capdevielle. CORSIKA: A Monte Carlo code to simulate extensive air showers. (Report:FZKA-6019), 1998.
- [12] Tetsufumi Hirano, Naomi van der Kolk, and Ante Bilandzic. Hydrodynamics and Flow. *Lect. Notes Phys.*, 785:139–178, 2010.
- [13] N. N. Kalmykov, S. S. Ostapchenko, and A. I. Pavlov. Quark-Gluon String Model and EAS Simulation Problems at Ultra-High Energies. *Nucl. Phys. Proc. Suppl.*, 52:17–28, 1997.
- [14] V. Khachatryan et al. Evidence for collective multiparticle correlations in p -Pb collisions. *Phys. Rev. Lett.*, 115:012301, Jun 2015.
- [15] Michael L. Miller, Klaus Reygers, Stephen J. Sanders, and Peter Steinberg. Glauber modeling in high energy nuclear collisions. *Ann. Rev. Nucl. Part. Sci.*, 57:205–243, 2007.
- [16] S. Ostapchenko. QGSJET-II: Towards reliable description of very high energy hadronic interactions. *Nucl. Phys. Proc. Suppl.*, 151:143–146, 2006.
- [17] Karl Pearson. On the theory of contingency and its relation to association and normal correlation. *Biometric Series No. 1*, 1904.
- [18] T. Pierog. Personal communication.
- [19] T. Pierog, Iu. Karpenko, J. M. Katzy, E. Yatsenko, and K. Werner. EPOS LHC: Test of collective hadronization with data measured at the CERN Large Hadron Collider. *Phys. Rev.*, C92(3):034906, 2015.
- [20] T. Pierog and K. Werner. EPOS Model and Ultra High Energy Cosmic Rays. *Nucl. Phys. Proc. Suppl.*, 196:102–105, 2009.

- [21] Jan Ridky. Can we observe the quark gluon plasma in cosmic ray showers? *Astropart. Phys.*, 17:355–365, 2002.
- [22] T. Pierog, C. Baus, and R. Ulrich. CRMC website. <https://web.iikp.kit.edu/rulrich/crmc.html>.
- [23] K. Werner, B. Guiot, Iu. Karpenko, and T. Pierog. Analysing radial flow features in p-Pb and p-p collisions at several TeV by studying identified particle production in EPOS3. *Phys. Rev.*, C89(6):064903, 2014.
- [24] K. Werner, B. Guiot, Iu. Karpenko, and T. Pierog. Flow in pPb collisions at 5 TeV? In *Proceedings, 49th Rencontres de Moriond on QCD and High Energy Interactions: La Thuile, Italy, March 22-29, 2014*, pages 309–314, 2014.
- [25] Klaus Werner. The hadronic interaction model EPOS. *Nucl. Phys. Proc. Suppl.*, 175-176:81–87, 2008.